ANTIOXIDANTS & REDOX SIGNALING
Volume 16, Number 12, 2012

DOI: 10.1089/ars.2011.4173

Mitochondrion-Derived Reactive Oxygen Species Lead to Enhanced Amyloid Beta Formation

Kristina Leuner,[1,2] Tanja Schütt,[1] Christopher Kurz,[1] Schamim H. Eckert,[1] Carola Schiller,[1] Angelo Occhipinti,[3,4] Sören Mai,[5] Marina Jendrach,[5] Gunter P. Eckert,[1] Shane E. Kruse,[6] Richard D. Palmiter,[6] Ulrich Brandt,[7] Stephan Dröse,[7] Ilka Wittig,[7] Michael Willem,[8,9] Christian Haass,[8,9] Andreas S. Reichert,[3,4] and Walter E. Müller[1]

Abstract

Aims: Intracellular amyloid beta (Aβ) oligomers and extracellular Aβ plaques are key players in the progression of sporadic Alzheimer's disease (AD). Still, the molecular signals triggering Aβ production are largely unclear. We asked whether mitochondrion-derived reactive oxygen species (ROS) are sufficient to increase Aβ generation and thereby initiate a vicious cycle further impairing mitochondrial function. ***Results:*** Complex I and III dysfunction was induced in a cell model using the respiratory inhibitors rotenone and antimycin, resulting in mitochondrial dysfunction and enhanced ROS levels. Both treatments lead to elevated levels of Aβ. Presence of an antioxidant rescued mitochondrial function and reduced formation of Aβ, demonstrating that the observed effects depended on ROS. Conversely, cells overproducing Aβ showed impairment of mitochondrial function such as comprised mitochondrial respiration, strongly altered morphology, and reduced intracellular mobility of mitochondria. Again, the capability of these cells to generate Aβ was partly reduced by an antioxidant, indicating that Aβ formation was also ROS dependent. Moreover, mice with a genetic defect in complex I, or AD mice treated with a complex I inhibitor, showed enhanced Aβ levels *in vivo*. ***Innovation:*** We show for the first time that mitochondrion-derived ROS are sufficient to trigger Aβ production *in vitro* and *in vivo*. ***Conclusion:*** Several lines of evidence show that mitochondrion-derived ROS result in enhanced amyloidogenic amyloid precursor protein processing, and that Aβ itself leads to mitochondrial dysfunction and increased ROS levels. We propose that starting from mitochondrial dysfunction a vicious cycle is triggered that contributes to the pathogenesis of sporadic AD. *Antioxid. Redox Signal.* 16, 1421–1433.

Introduction

Sporadic Alzheimer's disease (AD), the most common age-related neurodegenerative disease, is characterized by initial memory impairment progressing toward total loss of mental and physical abilities (17, 39, 46). The key histopathological features are amyloid-beta (Aβ) containing plaques and microtubule-associated tau-bearing neurofibrillary tangles. In contrast to familial AD caused by a mutation in the amyloid precursor protein (APP), or the presenilin genes 1 and 2 leading to increased Aβ load, the main risk factor for sporadic AD is aging itself (34, 38). Aging is associated with long-time exposure of our brain to oxidative stress, leading to accumulation of oxidized proteins, lipids, and nucleic acids. The mitochondrion, the major hub of cellular energy conversion, is a main source of reactive oxygen species (ROS) (35, 37). The majority of ROS derive from complexes I and III of the respiratory chain in the form of superoxide anion radicals (2, 27). Importantly, complex I activity declines substantially during normal brain aging, whereas complex III activity is

[1]Department of Pharmacology, ZAFES, Biocenter, University of Frankfurt, Frankfurt/Main, Germany.
[2]Molecular and Clinical Pharmacy, FAU Erlangen/Nürnberg, Erlangen, Germany.
[3]Mitochondrial Biology, Frankfurt Institute for Molecular Life Sciences, Frankfurt/Main, Germany.
[4]Mitochondrial Biology, Medical School, Goethe University, Frankfurt/Main, Germany.
[5]Kinematische Zellforschung, Biocenter, University of Frankfurt, Frankfurt/Main, Germany.
[6]Department of Biochemistry, Howard Hughes Medical Institute, University of Washington, Seattle, Washington.
[7]Molecular Bioenergetics Group, Cluster of Excellence Frankfurt "Macromolecular Complexes," Medical School, Johann Wolfgang Goethe-Universität, Frankfurt/Main, Germany.
[8]DZNE—German Center for Neurodegenerative Diseases, Munich, Germany.
[9]Biochemistry, Adolf-Butenandt-Institute, Ludwig-Maximilians-University, Munich, Germany.

Innovation

We show that mitochondrion-derived reactive oxygen species (ROS) trigger amyloid beta (Aβ) production. This may set off a vicious cycle of enhanced Aβ production in the progression of sporadic Alzheimer's disease (AD), since Aβ itself accelerates mitochondrial dysfunction and its own production *via* enhanced β-site APP cleaving enzyme 1 activity due to increased ROS levels (Fig. 8). This mechanism may help to explain why aging, which is strongly associated with mitochondrial dysfunction, is the major risk factor to develop sporadic AD.

nearly unchanged (2, 27, 32), suggesting complex I as the major player of the brain aging scenario. Not only in familial AD but also in sporadic AD, a gradual increase of Aβ levels over years or even decades is considered to play an important role in pathogenesis. Enhanced amyloidogenic processing of APP by the β-site APP cleaving enzyme (BACE) and the γ-secretase complex leads to increased intracellular levels of soluble oligomeric Aβ, resulting in pronounced synaptic failure and eventually in memory decline (17, 46). However, the mechanism by which APP processing is triggered in sporadic AD patients is still not known and probably represents one of the most important missing links in the understanding of this devastating disease.

Several recent findings show that mitochondrial dysfunction is one of the earliest pathogenic alterations in AD (11, 18, 44, 49). In post-mortem brain tissue of sporadic AD patients, a deficiency in cytochrome c oxidase (complex IV) activity is consistently reported (54). In several AD animal models, mitochondrial dysfunction resulting in decreased mitochondrial membrane potential (MMP), reduced ATP levels, declined complex IV activity, and enhanced oxidative stress was detected (18, 49). Furthermore, mitochondrial dynamics (fusion and fission) and morphology are altered in AD (47, 48, 52, 59). The aforementioned pathological changes are already observed when only oligomeric Aβ could be detected and fibrillar plaques were not yet present (18, 49, 61), stressing the early contribution of mitochondrial dysfunction to the progression of the disease. Here, we asked whether mitochondrial dysfunction, especially complex I dysfunction associated with enhanced ROS production, might be the initial trigger for altered APP processing, which in turn might result in a vicious cycle further impairing mitochondrial dysfunction, leading to apoptosis, synaptic dysfunction, and memory decline.

Results

Complex I dysfunction induced by rotenone leads to Aβ generation

As a simple experimental cell model for complex I dysfunction, we used the effects of the complex I inhibitor rotenone on mitochondrial function in HEK293 cells. Treatment with rotenone led to a significant reduction of MMP and ATP levels (Fig. 1A), and to a substantial increase in superoxide anion radicals and cytosolic ROS levels (Fig. 1B). MMP and ATP level constantly declined over 24 h (Supplementary Fig. S1A, B; Supplementary Data are available online at www.liebertonline.com/ars), whereas both superoxide anion radicals and cytosolic ROS levels reached a peak after 2 h (Supplementary Fig. S1C, D). Furthermore, rotenone treatment induced pronounced mitochondrial fragmentation (Fig. 1C, D). These experiments confirm earlier studies (4, 22, 57) that rotenone as applied here induced mitochondrial dysfunction and increased mitochondrion-derived ROS formation. Next we asked whether complex I dysfunction is sufficient to induce enhanced Aβ generation. A$\beta_{1\text{-}40}$ levels were determined after 2 h when ROS levels were maximally elevated and after 24 h when MMP, ATP, and mitochondrial morphology were significantly impaired. As early as 2 h after the insult with rotenone, A$\beta_{1\text{-}40}$ levels were modestly increased (Fig. 2A). After 24 h this effect was much more pronounced and A$\beta_{1\text{-}40}$ levels were significantly increased by 75% compared to unstressed control cells (Fig. 2A). The levels of A$\beta_{1\text{-}42}$ production at the scale of these experiments were too low for a reliable detection even after inhibiting complex I.

Complex I-induced Aβ increase is mediated by enhanced ROS level

To elucidate the mechanism responsible for complex I-induced increased Aβ generation, we investigated whether elevated ROS levels are the trigger for altered APP processing. To test this hypothesis the antioxidant vitamin C was used to scavenge ROS. To determine the active antioxidant concentration, first the effects of different vitamin C concentrations (1–1000 μM) on the levels of superoxide anion were tested. HEK293 cells were preincubated with vitamin C for 4 h, rotenone 25 μM was added, and dihydroethidium (DHE) fluorescence was measured after 2 h when maximal superoxide anion radical levels were detected after rotenone insult. Vitamin C at a concentration of 1000 μM reduced superoxide anion radicals by about 25% after rotenone treatment (Fig. 2B). Next we investigated whether vitamin C was sufficient to reduce rotenone-induced Aβ formation. Indeed, vitamin C at the concentration that reduced ROS levels by about 25% was sufficient to reduce A$\beta_{1\text{-}40}$ levels by about 20% (Fig. 2C). This effect was accompanied by a protection against mitochondrial fragmentation (Fig. 2D, E). Taken together, these experiments demonstrate that triggering the formation of Aβ can be suppressed by scavenging complex I-derived ROS.

Complex III-derived ROS also results in increased Aβ production

To define whether these findings are an effect specifically mediated *via* complex I-derived ROS or whether ROS generation by complex III, the second key player generating mitochondrial ROS, might also trigger Aβ production, the complex III inhibitor antimycin was administered and the effects on superoxide anion radical levels and soluble A$\beta_{1\text{-}40}$ were examined (Fig. 3). DHE fluorescence in HEK293 cells increased significantly over a period of 120 min (Fig. 3A). Similarly to rotenone, antimycin also increased the levels of soluble A$\beta_{1\text{-}40}$ modestly after 2 h and significantly after 24 h (Fig. 3B). We conclude that both complex I- and complex III-derived ROS trigger formation of Aβ.

Aβ overproduction impairs mitochondrial function and mitochondrial dynamics

To simulate increased Aβ levels during the progression of sporadic AD, HEK293 control cells that stably overexpress

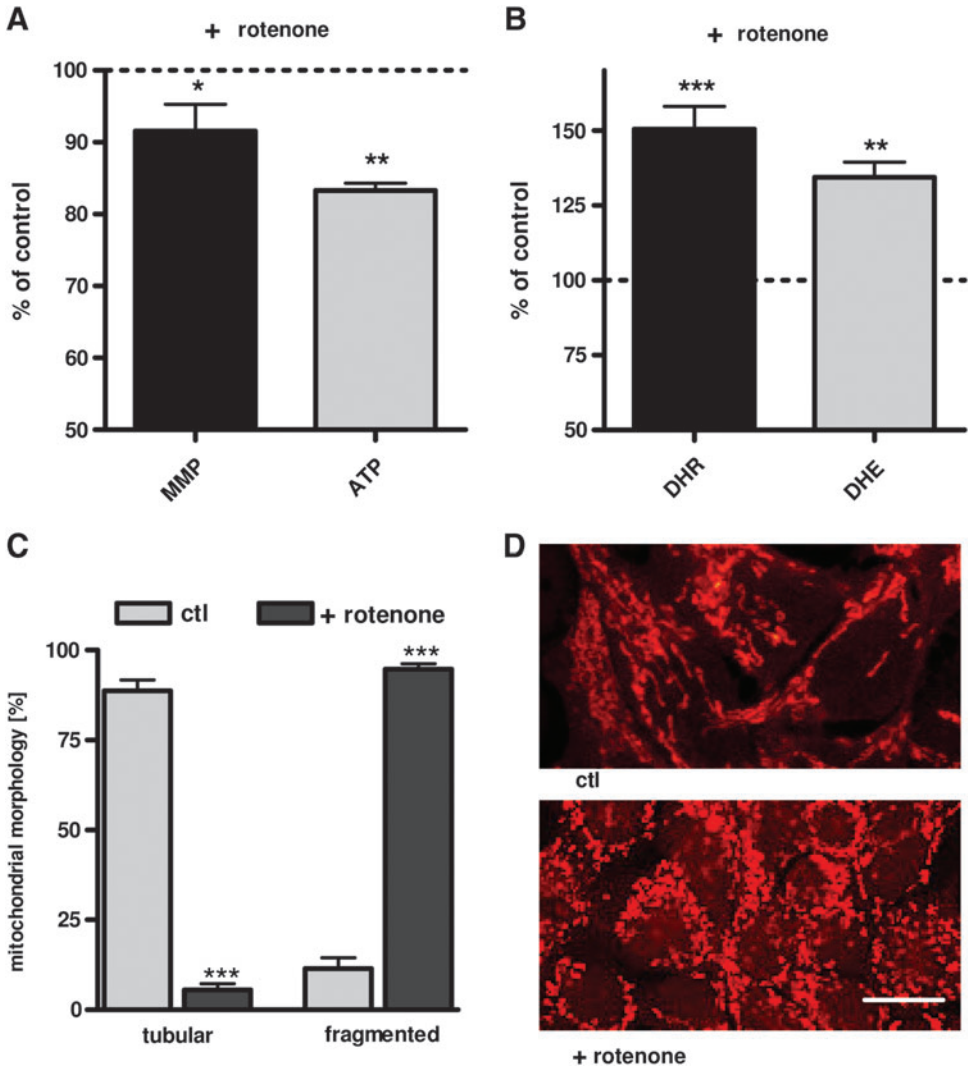

FIG. 1. Complex I inhibitor rotenone leads to mitochondrial dysfunction, fragmentation, and enhanced reactive oxygen species (ROS) production. (A) Mitochondrial membrane potential (MMP; R123 mean fluorescence intensity [MFI] normalized on% of untreated control) and ATP levels were significantly reduced after 24-h treatment with rotenone (25 μM). **(B)** Levels of superoxide anion radicals (dihydroethidium [DHE] fluorescence normalized on% of untreated controls), and cytosolic ROS (dihydrorhodamin [DHR] fluorescence protein normalized on% of untreated controls) were increased after 2 h treatment with rotenone (25 μM). **(C)** Histogram of quantitative analysis of mitochondrial morphology (Mitotracker CMXRos) after 24 h rotenone insult (100 mitochondria/n). **(D)** Representative confocal images that revealed changes in the mitochondrial morphology of human embryonic kidney (HEK) cells treated with rotenone (25 μM, 24 h; bars represent 10 μm) compared to untreated controls after mitochondrial staining with MitoTracker CMXRos (*red*). **(A–C)** $n = 6 \pm$ standard error of the mean (SEM); unpaired t-test; $^{*}p < 0.05$, $^{**}p < 0.01$, $^{***}p < 0.001$. (To see this illustration in color the reader is referred to the web version of this article at www.liebertonline.com/ars).

either wild-type APP (APPwt) or the Swedish mutation (APPsw) were used to elucidate the effects of enhanced Aβ levels on mitochondrial function and ROS production. The cells were characterized by different $A\beta_{1\text{-}40}$ loads increasing from control cells (untransfected human embryonic kidney cells [HEKut]), to APPwt to APPsw cells (Fig. 4A). Using APPwt or APPsw cell lines allowed us to study the dose-dependent effects of Aβ, both representing a model of chronic Aβ stress characterized by $A\beta_{1\text{-}42}/A\beta_{1\text{-}40}$ ratios of 1/100 in APPwt and 1/1000 in APPsw cells. Superoxide anion radials were increased to a similar extent in APPwt and APPsw cells (Fig. 4B) although $A\beta_{1\text{-}40}$ levels were 100-fold higher in APPsw cells than in APPwt cells (Fig. 4B). Comparing $A\beta_{1\text{-}40}$, ATP levels (Fig. 4C), MMP (Fig. 4E), and cell viability (Fig. 4D) were significantly impaired in both cell types compared with control cells. To assess the capacity of the entire oxidative phosphorylation system (Fig. 4F), the respiratory control ratio (RCR) was determined by dividing basal respiration by respiration in the presence of the complex V inhibitor oligomycin as an indicator of the state of coupling (21). A significant reduction in RCR was detected in APPwt and APPsw cells, which was consistent with reduced ATP levels in APPwt and APPsw cells (Fig. 4F).

We further characterized mitochondrial function in these cells by analyzing mitochondrial morphology and dynamics (Fig. 5A–C). Cells overexpressing APP demonstrate a significantly increased fraction of fragmented mitochondria (Fig. 5A, B). Further, live-cell imaging of MitoTracker Deep

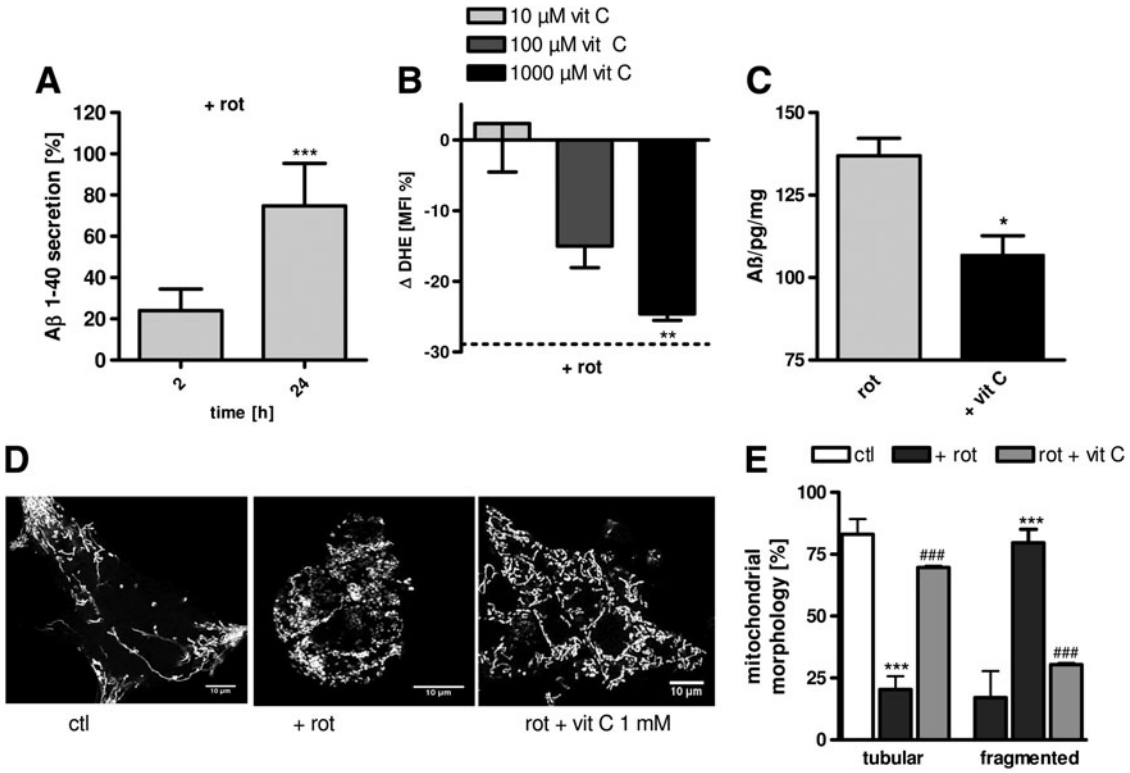

FIG. 2. Complex I dysfunction leads to ROS-dependent Aβ generation. (A) Soluble $A\beta_{1\text{-}40}$ levels in HEK cells are significantly increased after 24-h insult with rotenone (rot; 25 μM) compared to control cells (ctl). **(B)** 4-h preincubation with vitamin C (1000 μM) leads to a significant reduction of superoxide anion radicals (Δ DHE MFI, normalized on % of untreated controls) after rotenone insult (25 μM, 2 h). **(C)** ROS scavenging using vitamin C (1000 μM) results in significantly reduced $A\beta_{1\text{-}40}$ levels after 24 h insult with rotenone (25 μM). **(D)** Representative images reveal changes in mitochondrial morphology when cells are pretreated with vitamin C (1000 μM) and afterward stressed with rotenone (25 μM) compared to untreated controls. Mitochondria were stained with MitoTracker CMXRos (bars represent 10 μm). **(E)** Histogram of quantitative analysis of mitochondrial morphology in the presence and absence of vitamin C (1000 μM, preincubation 4 h) after 24-h rotenone insult (100 mitochondria/n). **(A–C)** $n = 6 \pm$ SEM; unpaired t-test; $^{*}p < 0.05$, $^{**}p < 0.01$, $^{***}p < 0.001$. **(E)** $n = 6 \pm$ SEM; unpaired t-test, $^{***}p < 0.001$ ctl compared to rotenone treated cells, $^{\#\#\#}p < 0.001$ rotenone treated cells against vit C + rotenone-treated cells.

Red–stained mitochondria was performed for 2 min and the mobility of mitochondria as revealed by the average change in mitochondrial localization was determined. The APPwt and APPsw cells exhibited a slight but significant reduction of mitochondrial mobility compared to control cells (Fig. 5C).

Taken together, mitochondrial function and the extent of ROS formation is affected to a similar extent in APPwt and APPsw cells when compared to control cells. These results indicate that deterioration of mitochondrial functionality might already be promoted at moderately elevated Aβ levels and does not further increase with higher Aβ levels such as those present in APPsw cells. This might be a relevant finding for disease progression in sporadic AD, since it suggests that moderate elevation of Aβ can be sufficient to impair mitochondrial function already at early stages of AD.

Involvement of ROS in Aβ-mediated mitochondrial dysfunction

BACE1, together with a disintegrin and metalloprotease domain (ADAM) and γ-secretase, regulates APP processing (17). To test whether elevated Aβ levels are only due to the overexpression of APPwt or APPsw, or if other mechanisms such as mitochondrial dysfunction and elevated ROS are also involved, APPwt and APPsw cells were treated with vitamin C, and ROS levels, $A\beta_{1\text{-}40}$, and BACE1 activity were investigated. We focused on BACE1 activity because BACE1 activity was earlier shown to increase upon applying external oxidative stress using H_2O_2 (55). BACE1 activity was two- to threefold increased in both APPwt and APPsw cells compared to control cells (Fig. 6A). To investigate the possible role of increased ROS levels, vitamin C was used and its effects on superoxide anion radicals, BACE1 activity, and Aβ levels were tested. APPwt and APPsw cells were incubated for 24 h with vitamin C (1000 μM) (Fig. 6). Superoxide anion radicals were significantly reduced in both cell types (Fig. 6B) and BACE1 activity was significantly diminished (Fig. 6C). In addition, Aβ levels were moderately reduced in APPwt cells and significantly reduced in APPsw cells (Fig. 6D). We conclude that altered APP processing promoting Aβ formation is at least in part linked to ROS-dependent BACE1 activity.

Mitochondrial dysfunction leads to increased Aβ production in vivo

After demonstrating that complex I dysfunction leads *via* enhanced ROS production to elevated Aβ levels and that Aβ itself further impairs mitochondrial function, we asked whether these findings could be confirmed in a neuronal cell line and two mouse models. In SH-SY5Y cells, a dose-dependent

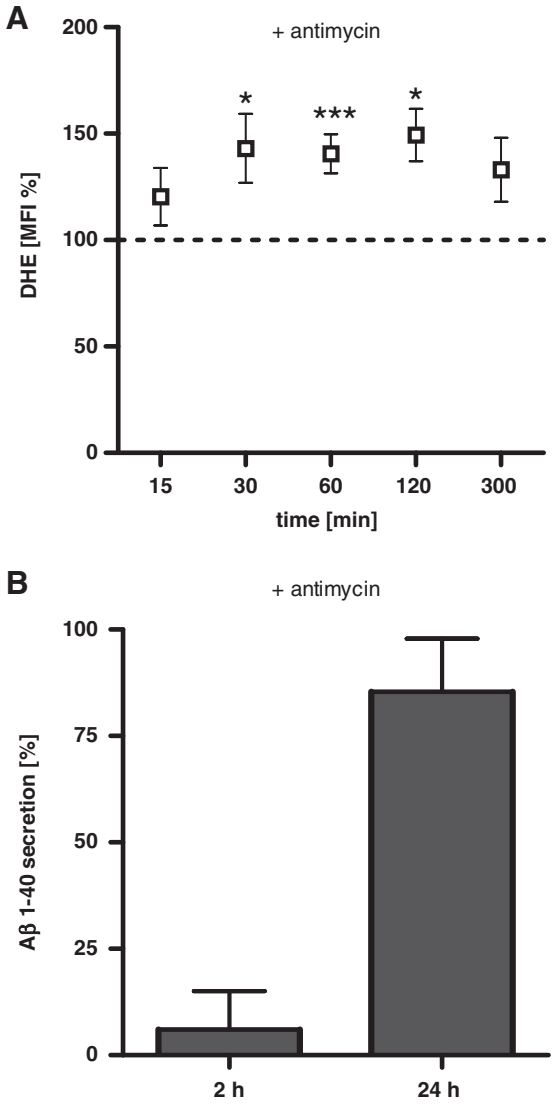

FIG. 3. Complex III dysfunction also leads to enhanced ROS and Aβ levels. (A) Levels of superoxide anion radicals (DHE MFI normalized on untreated controls) were significantly increased after the treatment with antimycin (100 μM) for 30, 60, and 120 min. **(B)** Soluble A$\beta_{1\text{-}40}$ levels in HEK cells are significantly increased after 24-h insult with antimycin (100 μM) compared to cells without antimycin. **(A, B)** $n = 6 \pm$ SEM; unpaired *t*-test; $^*p < 0.05$, $^{***}p < 0.001$.

effect of rotenone was observed on MMP and ATP levels as well as on A$\beta_{1\text{-}40}$ levels (Fig. 7A, B). Already at a concentration of 2.5 μM rotenone, a significant decrease of ATP and MMP was detected, which correlated with enhanced soluble A$\beta_{1\text{-}40}$ levels. A maximal effect was measured at a concentration of 25 μM rotenone, which was in agreement with the effect of rotenone in HEK cells. Our data are consistent with the findings reported in fibroblasts, where rotenone leads to maximally increased ROS levels and a reduction of complex I activity only at concentrations in the micromolar range (57).

Moreover, we used a mouse model with complex I deficiency due to inactivation of the *Ndufs4* gene (complex I subunit) first described by Kruse *et al.* (2008). We determined soluble A$\beta_{1\text{-}40}$ levels in whole brain homogenates of 5-week-old homozygous knockout (KO) *Ndufs4* KO mice compared to age-matched heterozygous and wild-type *Ndufs4* mice. The KO mice have reduced complex I activity. Until week 5 they appear healthy, then ataxia progresses until death at week 7 (8, 26). Mice heterozygous for Ndufs4 are indistinguishable in behavior compared to wild-type mice. In this genetic model of complex I dysfunction, soluble A$\beta_{1\text{-}40}$ levels in brain homogenates were significantly enhanced in KO mice compared to heterozygous (het) and wild-type (wt) mice (Fig. 7C).

To further corroborate our results, we decided to treat mice representing a well-established mouse model for AD with the complex I inhibitor rotenone. C57BL/6 mice bearing the human Swedish (S:KM595/596NL) and London (L:V717I) mutations in the 751 amino acid form of human APP (tgAPP) under the control of a murine Thy-1 promoter at an age of 13 months. Age-matched nontransgenic littermate animals were treated for 3 days with rotenone i.p. (10 mg/kg/body weight [BW]) and soluble Aβ levels in brain homogenates were investigated. Again, A$\beta_{1\text{-}40}$ levels were increased in animals treated with rotenone compared to animals only receiving the vehicle (Fig. 7D). These results strongly support our hypothesis that mitochondrial dysfunction associated with elevated ROS, in particular complex I dysfunction, induces enhanced amyloidogenic APP processing resulting in elevates Aβ levels.

Discussion

Our study provides several lines of evidence that mitochondrion-derived ROS are a sufficient trigger for inducing formation of Aβ. This may have major implications as it suggests that mitochondrial dysfunction is involved early in the pathogenesis of sporadic AD (Fig. 8). This view fits to the fact that mitochondrial dysfunction associated with enhanced mitochondrial ROS production is considered to be intimately involved in the aging process (5). Mitochondria are a major source and target of ROS produced by the respiratory chain that attack mitochondrial constituents, including proteins, lipids, and mtDNA (37). The two major sites of oxidative stress generation are complex I and complex III (40, 41, 45). Mainly, complex I is specifically susceptible to the aging process because 7 of 13 mt-DNA encoded polypeptides acting as subunits of respiratory chain complexes are found in complex I (43). A progressive alteration of mitochondrial gene expression was observed in rats and humans, including the NDUFV1 subunit of complex I, which is involved in electron transfer (6, 30).

On the basis of the following arguments, we hypothesize that complex I dysfunction associated with increased ROS production is a starting point and driving force of the amyloid cascade in AD. First, complex I dysfunction was induced in HEK293 cells with the complex I inhibitor rotenone leading to severe mitochondrial dysfunction, increased ROS, a fragmentation of mitochondria, and significantly increased soluble A$\beta_{1\text{-}40}$ levels. This increase could be attenuated by scavenging of ROS with vitamin C, which also improved mitochondrial morphology showing that mitochondrion-derived ROS contribute to amyloidogenic APP processing. The group of Palmiter recently published an effect of rotenone on microtubule depolymerization that was independent of complex I (8). However, we primarily consider rotenone-induced ROS formation as relevant for our findings since increasing ROS levels by complex III inhibition with antimycin A also leads to significantly increased Aβ levels. Our findings that ROS are involved in enhanced APP processing are

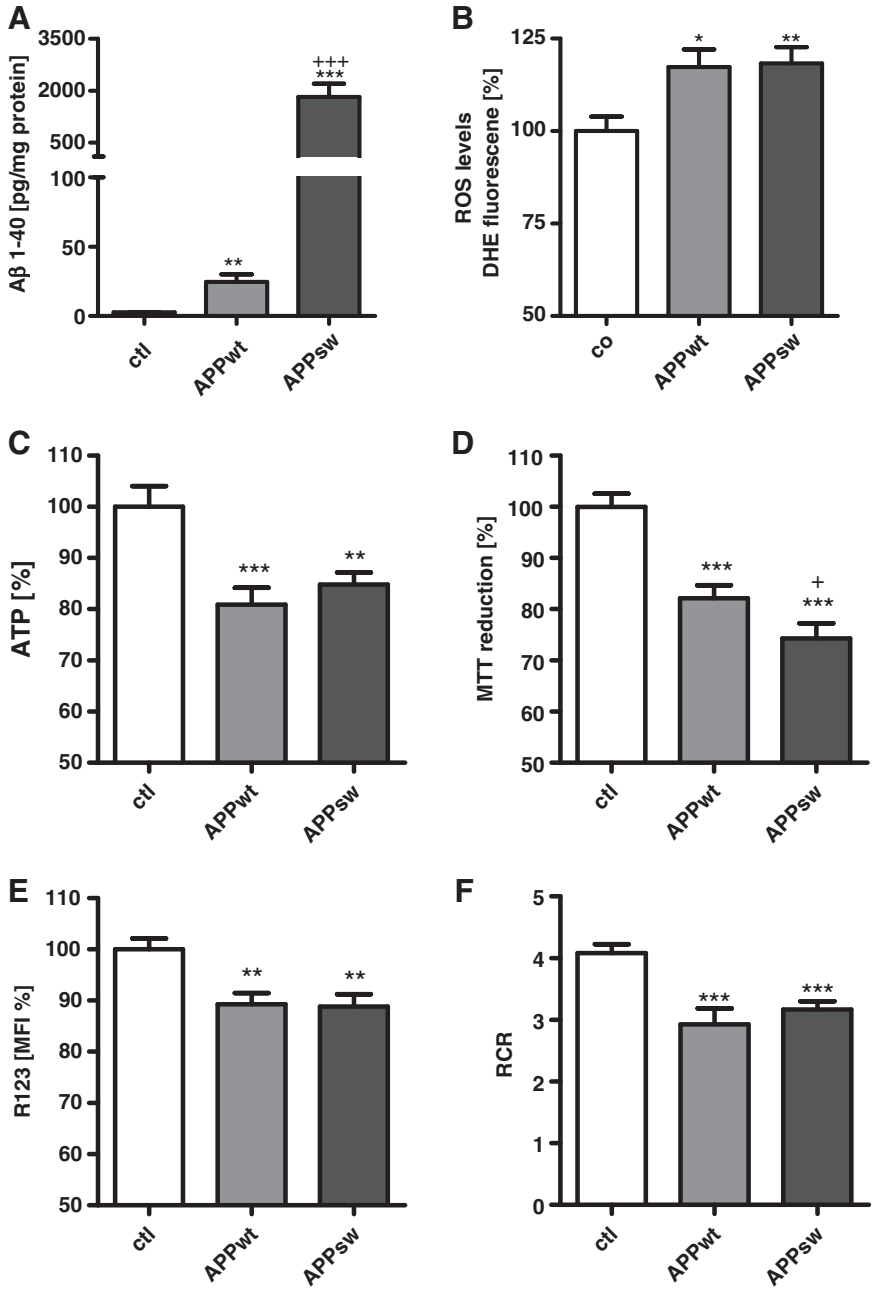

FIG. 4. Mitochondrial function is greatly impaired in wild-type amyloid precursor protein (APPwt) and APP containing the Swedish mutation (APPsw) cells. (A) $A\beta_{1\text{-}40}$ levels in transfected HEK cells are significantly increased in APPwt and APPsw cells. **(B)** Superoxide anion radicals (DHE fluorescence units/mg protein normalized on control cells) are significantly enhanced in APPwt and APPsw cells. **(C)** ATP levels and cell viability **(D)** are reduced in both APPwt and APPsw. **(E)** MMP (R123 units/mg protein expressed as MFI normalized to control cells) is significantly impaired in APPwt and APPsw cells. **(F)** Using a high-resolution respiratory system, respiratory control ratio (RCR; basal respiration/respiration under the treatment with oligomycin) representing the mitochondrial coupling state is significantly reduced again in APPwt and APPsw cells **(A–E)** $n = 6 \pm$ SEM; unpaired *t*-test; ctl against APPwt or APPsw $^{*}p < 0.05$, $^{**}p < 0.01$, $^{***}p < 0.001$. $^{+}p < 0.05$ APPwt against APPsw, $^{+++}p < 0.001$ APPwt against APPsw.

supported by earlier findings demonstrating that H_2O_2 also induced elevated Aβ levels (16, 55). Furthermore, hypoxia and energy deprivation that are also associated with enhanced ROS levels as well lead to increased Aβ levels in cell and mouse models (42, 53).

To explore if Aβ itself can cause mitochondrial dysfunction and oxidative stress and thereby may start a vicious cycle accelerating amyloidogenic APP processing, HEK293 cells overexpressing human APPwt, and the APPsw mutation were used. APPwt cells reflect the physiological situation during aging with moderately elevated Aβ levels and APPsw, the scenario occurring in the familial AD with high Aβ levels. Mitochondrial function was broadly disturbed in both cell types as reflected by reduced MMP, decreased ATP levels, declined RCR, increased ROS levels, and altered mitochondrial morphology and mobility. Our findings are in line with recent studies in animal and cell models of AD (18, 25, 49, 61), which also showed a decrease in MMP and ATP levels. Complex IV activity is specifically attenuated by Aβ. In addition, others and we showed that complex I activity is synergistically downregulated by Aβ and tau to the already impaired complex I activity during aging (9, 18, 49). In both cases, expression of different subunits of complexes I and IV is deregulated (49). Decreased expression levels may be further result from the interaction of Aβ with the translocase of the outer mitochondrial membrane (TOM) (10) as Aβ has been proposed to block TOM and thereby the import of nuclear encoded proteins important for the respiratory chain (1). Furthermore, we observed mitochondrial fragmentation, and reduced mitochondrial mobility in APPwt and APPsw cells pointing to an imbalance in mitochondrial fission and fusion processes. These findings are in line with experiments

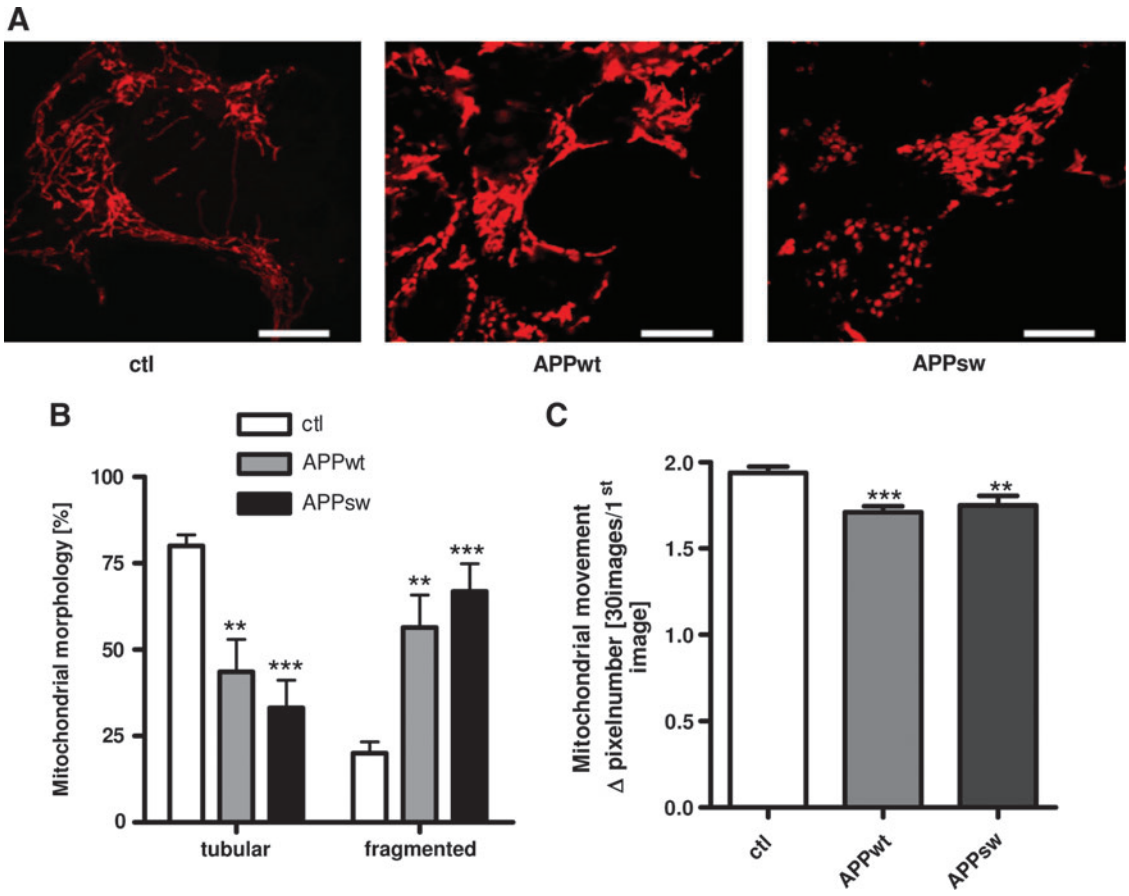

FIG. 5. Mitochondrial morphology is strongly altered in APPwt and APPsw cells. (A) Representative example of confocal microscopic images revealing mitochondrial morphology changes in APPwt and APPsw cells. Mitochondrial staining was done using MitoTracker CMXRos (*red*, bars represent 10 μm). **(B)** Histogram of mitochondrial morphology quantification (100 mitochondria/n were analyzed). **(C)** Live cell imaging of mitochondria stained with MitoTracker Deep Red. Images were recorded over 2 min (one picture every 1.5 s) to study mitochondrial dynamics. Histogram depicting quantitative changes in mitochondrial dynamics in APPwt and APPsw cells. **(B, C)** $n = 6 \pm$ SEM; unpaired t-test; $^{**}p < 0.01$, $^{***}p < 0.001$ ctl against APPwt or ctl against APPsw, respectively. (To see this illustration in color the reader is referred to the web version of this article at www.liebertonline.com/ars).

showing that oligomeric Aβ leads to mitochondrial fragmentation and increased fission associated by an increased expression of fission factors such as DRP-1 (51, 52, 58, 59).

Importantly, in our cell model moderately elevated Aβ levels are sufficient to induce mitochondrial dysfunction. There seems to be a maximal effect on mitochondrial function already observed in APPwt cells, which have much lower Aβ levels than APPsw cells. These findings could explain why moderately enhanced Aβ levels due to mitochondrial dysfunction during aging are sufficient to initiate the pathological cascade of sporadic AD.

In addition, we found that ROS levels and BACE1 activity were significantly increased in APPwt and APPsw cells. The connection between elevated oxidative stress and increased Aβ production in HEK control cells, APPwt, and APPsw cells was further supported by elevated $A\beta_{1\text{-}40}$ levels after the treatment with H_2O_2 (Supplementary Fig. S2). Importantly, ROS scavenging leads to reduced Aβ levels and BACE1 activity. The enhanced oxidative stress in this AD cell model is presumably caused by two different mechanisms: (1) impairment of complex I activity directly by Aβ (18, 49) and (2) the induction of oxidative stress by Aβ aggregation itself (33, 46). Transition metals such as Cu^{2+}, Zn^{2+}, or Fe^{3+} enhance Aβ neurotoxicity by producing H_2O_2. These findings are supported by several groups using different AD models (3, 18, 25, 36, 46, 49). Furthermore, our findings are consistent with earlier reports in which H_2O_2, energy deprivation, or ischemia, stressors that are known to cause elevated ROS levels, increase the activity and the expression levels of BACE1 (55, 56). Importantly, elevated BACE1 activity after ischemia was reversed by the antioxidant trolox or superoxide dismutase overexpression (16). At the signal transduction level, the c-jun N-terminal kinase/c-jun pathway is discussed to be key player to regulate BACE1 expression after oxidative stress (55).

BACE1 regulates, together with ADAM and γ-secretase, APP processing. Increased BACE1 activity was proposed to be linked to AD (20, 28, 60). Overexpression of the enzyme was demonstrated to dramatically increase Aβ production, while a knock-down of BACE1 is associated with reduced Aβ generation (7, 31). Furthermore, BACE1 protein was found to be increased in frontal cortex of AD patients compared to controls (19). In addition, an increase of γ-secretase was found in temporal cortex of AD patients (15). Taken together, we propose

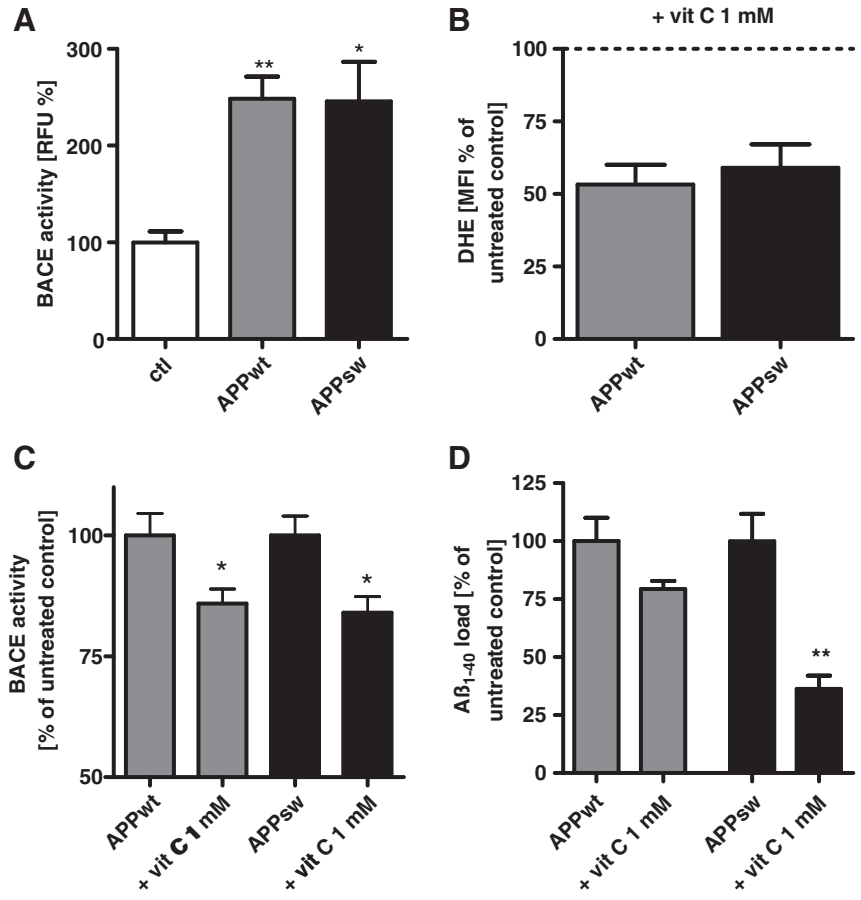

FIG. 6. ROS are also involved in amyloidogenic APP processing in APPwt and APPsw cells. (A) Basal β-site APP cleaving enzyme 1 (BACE1) activity is increased in APPwt and APPsw cells. **(B)** Effectivity of ROS scavenging in APPwt and APPsw cells by vitamin C on DHE MFI (1000 μM; 4 h incubation). **(C)** BACE1 activity is reduced in APPwt and APPsw cells by 4-h incubation of vitamin C (1000 μM). **(D)** Reduction of Aβ levels in APPwt and APPsw cells by vitamin C (1000 μM, 4 h incubation). **(A–D)** $n = 6 \pm$ SEM; unpaired t-test; $^*p < 0.05$, $^{**}p < 0.01$. **(A)** ctl against APPwt or ctl against APPsw. **(C, D)** APPwt or APPsw against APPwt + vit C or APPsw against APPsw + vit C.

that one possible mechanism explaining enhanced Aβ formation is linked to the ROS-dependent activation of BACE1.

To further test our hypothesis that mitochondrial dysfunction and especially complex I dysfunction is the starting point of the amyloid cascade in sporadic AD, we used SH-SY5Y cells as a neuronal cell model and two mouse models of complex I dysfunction. In SH-SY5Y cells, we found similar effects of rotenone on Aβ levels and mitochondrial function. In our first mouse model, which was deficient in complex I due to inactivation of the *Ndufs4* gene (22), Aβ levels were increased even before there was notable pathology or behavioral effects. Interestingly, in an AD animal model crossed with a complex IV KO model, Aβ levels were not increased, but, on the contrary, amyloid plaques were even reduced (14). This reduction is accompanied by a reduction in BACE1 activity, and ROS levels. These findings strongly suggest that not dysfunction of mitochondrial complexes *per se* is sufficient to induce Aβ elevation but that the mitochondrion-derived ROS mediate this deleterious effect.

In the second mouse model we used, Thy-1 APP mice treated with rotenone for 3 days, A$\beta_{1\text{-}40}$ levels were increased. These results are in line with recently published findings showing that in APP transgenic mice (Tg2576) the pesticide paraquat, which enhances ROS levels, also increases Aβ levels.

Not only in sporadic AD but also in sporadic Parkinson disease (PD), aging is the most prominent risk factor. We suggest that in both pathologies, complex I dysfunction that is tightly associated with aging plays an important role in the pathogenesis of these disorders. Several patients suffer from mixed forms of PD and AD associated with not only α-synuclein but also Aβ plaques. This could be explained by the mechanism proposed here. Disease-specific pathological features such as the APOE4 status in AD or the high sensitivity of substantia nigra neurons in PD might then trigger further progression of the respective neurodegenerative disease.

An important question that arises from our data is whether patients suffering from mitochondrial disorders such as mitochondrial encephalopathy, lactatacidosis, stroke-like episodes (MELAS), myoclonic epilepsy with ragged red fibers, or Kearns Sayre syndrome show cognitive decline and dementia (mitochondrial dementia). Indeed, cognitive impairment and dementia are frequent findings in mitochondrial disorders. Several clinical, morphological, functional, and chemical manifestations were detected in these patients (13). Recently, a sporadic case of progressive cognitive and behavioral decline was identified in patient with a rare m.3291T > C MELAS mutation (50). Interestingly, AD-like Aβ plaques were found in a female MELAS patient, who was only 54 years old at the time of testing, even though no evidence for familiar AD resulting from APP mutations was found (24).

Materials and Methods

Materials

Rhodamine 123 (R123), DHE, dihydrorhodamin (DHR), Mitotracker CMX ROS, Mitotracker Deep Red, and MTT were purchased from Invitrogen. Rotenone, antimycin, and ascorbic acid were obtained from Sigma. The ViaLight Plus assay

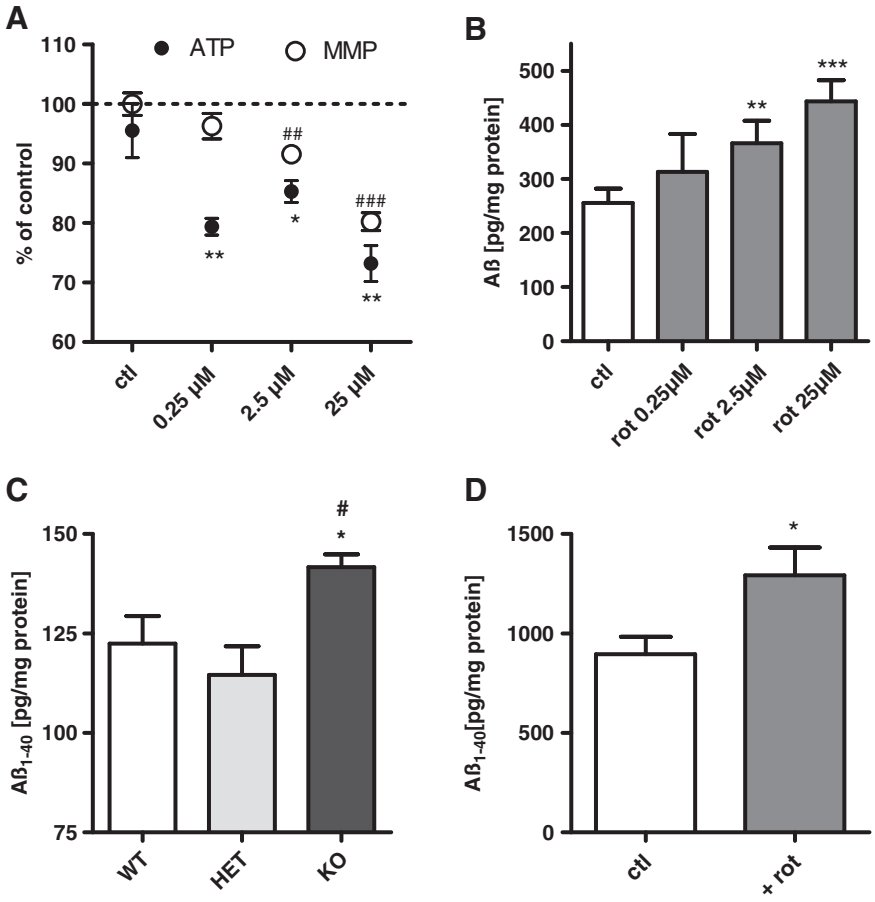

FIG. 7. Enhanced Aβ levels in a neuronal cell model and two animal models of complex I dysfunction. (A) SH-SY5Y cells were treated with rotenone (0.25, 2.5, and 25 μM) for 24 h and ATP and MMP as well as soluble $A\beta_{1\text{-}40}$ levels **(B)** were determined $n = 6 \pm$ SEM, unpaired *t*-test, **(A)** $^{*}p < 0.05$, $^{**}p < 0.01$, ATP ctl against rot, $^{\#\#}p < 0.01$, $^{\#\#\#}p < 0.001$ MMP against rot. **(B)** $^{**}p < 0.01$ ctl against rot 2.5 μM, $^{***}p < 0.001$ ctl against rot 25 μM. **(C)** APP transgenic animals received rotenone *via* i.p. application (10 mg/kg/body weight) or vehicle for 3 days and soluble $A\beta_{1\text{-}40}$ levels in brain homogenates were measured. $n = 6 \pm$ SEM per treatment group unpaired *t*-test $^{*}p < 0.05$. **(D)** In homozygous knockout (KO) *Ndufs4* mice, $A\beta_{1\text{-}40}$ levels are significantly increased compared to wild-type (wt) and heterozygous (HET) mice. Ndufs4 mice wt $n = 5 \pm$ SEM, HET $n = 5 \pm$ SEM, KO $n = 12 \pm$ SEM; unpaired *t*-test; $^{*}p < 0.05$ wt against KO, $^{\#}p < 0.05$ HET against KO.

was purchased from Lonza. Mouse $A\beta_{1\text{-}40}$, human $A\beta_{1\text{-}40}$, and $A\beta_{1\text{-}42}$ enzyme-linked immunosorbent assay (ELISA) were obtained from Invitrogen. The BACE activity assay was purchased from Calbiochem.

Cell culture

HEK cells were transfected with DNA constructs harboring the human mutant APP (APPsw, K640/n671L) gene, and the APPwt gene, inserted downstream of a cytomegalovirus promotore using the FUGENE 6 technology (Roche Diagnostics) (12, 25). The stably expressing APPwt and APPsw HEK 293 cells were cultured in Dulbecco's modified Eagle's medium supplemented with 10% heat-inactivated fetal calf serum, 50 units/ml penicillin and 50 μg/ml streptomycin, and 400 μg/ml G418 at 37°C in a humidified incubator containing 5% CO_2. HEKut cells were grown in Dulbecco's modified Eagle's medium supplemented with 10% heat-inactivated fetal calf serum, 50 units/ml penicillin, and 50 μg/ml streptomycin at 37°C in a humidified incubator containing 5% CO_2.

SH-SY5Y cells were grown in Dulbecco's modified Eagle's medium supplemented with 10% heat-inactivated fetal calf serum, 5% heat-inactivated horse serum, 50 units/ml penicillin, and 50 μg/ml streptomycin at 37°C in a humidified incubator containing 5% CO_2.

Fluorescence-activated cell sorting measurement

HEK cells were seeded at a density of 10^5 cells/well the day before the experiment in 48-well plates. They were incubated for 0.5, 1, 2, 5, or 24 h with rotenone (25 μM) at 37°C in culture medium at pH 7.4 and 37°C. Superoxide anion radical concentration was investigated after incubation with 5 μM DHE for 30 min. Other ROS species were detected after 15-min incubation with 10 μM DHR. After incubation with the fluorescence dyes, cells were washed with Hanks' balanced salt solution (HBSS) containing 138 m*M* NaCl, 6 m*M* KCl, 1 m*M* $MgCl_2$, 2 m*M* $CaCl_2$, 5.5 m*M* glucose, and 10 m*M* HEPES (pH 7.4, 37°C). Afterward, cells were resuspended in HBSS and immediately analyzed by flow cytometry (FACS Calibur; BD Bioscience) using Cell Quest pro software (BD Biosciences).

ATP assay

HEKut, HEK APPwt, HEK APPsw, and SH-SY5Y cells were plated the day before at a density of 2×10^4 cells/well in a white 96-well plate. HEKut cells were incubated with rotenone (25 μM) for 0.5, 1, 2, 5, or 24 h at 37°C in culture medium at pH 7.4 and 37°C. SH-SY5Y cells were incubated for 24 h with rotenone (0.25, 2.5, and 25 μM). Afterward, cells were washed twice with HBSS and the reagents were added according to the ViaLight Plus protocol. The bioluminescent method (ViaLight Plus Kit; Lonza) utilizes an enzyme, luciferase, which catalyzes the formation of light from ATP and luciferin. The emitted light is linearly related to the ATP concentration and is measured using a luminometer (Victor^2 multiplate reader; PerkinElmer Life Sciences).

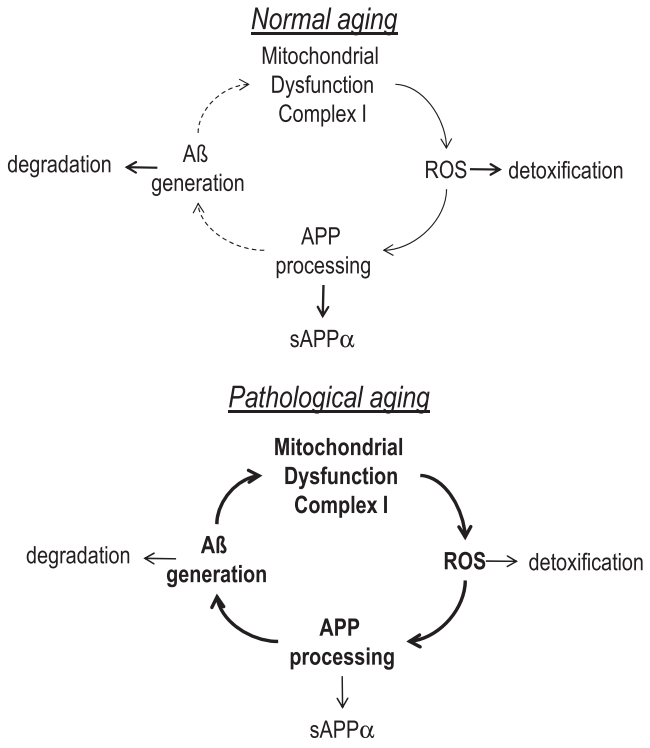

FIG. 8. Schematic illustration of mitochondrial dysfunction in healthy brain aging and pathological brain aging. In normal brain aging there is an equilibrium between mitochondrion-derived ROS, APP processing, and Aβ generation on the one hand and detoxification and degradation mechanisms on the other hand. During the disease process this balance is shifted toward the toxic mechanism with preponderance for mitochondrion-derived ROS, APP processing associated with increase BACE activity, and Aβ generation.

Determination of MMP

HEKut, HEK APPwt, HEK APPsw cells, and SH-SY5Y cells were plated the day before at a density of 2×10^5 cells per well in a 24-well plate. HEK ut cells were incubated for 0.5, 1, 2, 5, or 24 h at 37°C in culture medium at pH 7.4 and 37°C. SH-SY5Y cells were incubated for 24 h with rotenone (0.25, 2.5, and 25 μM). The MMP of HEK cells and SH-SY5Y cells was measured using the fluorescence dye R123. The experimental conditions used have been shown previously to detect even small changes (16, 21). Transmembrane distribution of the dye depends on the MMP. The dye was added to the cell culture medium in a concentration of 0.4 μM for 15 min (21). The cells were washed twice with HBSS and the fluorescence was determined with a fluorescence reader (Victor® multilabel counter; Perkin-Elmer) at 490/535 nm.

MTT assay

HEK cells were plated the day before at a density of 2×10^4cells/well in a 96-well culture plate. The assay is based on the cleavage of the yellow tetrazolium salt MTT into purple formazan by metabolically active cells. This cellular reduction involves the pyridine nucleotide cofactors NADH and NADPH. Twenty microliters (final concentration 1.0 mg/ml) of MTT reagent was added 2 h before the end of incubation. The formazan crystals were solubilized by adding 100 μl of a 20% sodium dodecyl sulfate/50% *N*,*N*-dimethly-formamide solution. The absorption of the solubilized formazan was measured at 570 nm using a microplate reader.

Mitochondrial respiration

HEK cells were harvested from culture plates, counted, adjusted to 3×10^6 cells per 2 ml in 37°C tempered cell medium, and transferred to the chamber of the Oxygraph2k from Oroboros Instruments. The cells were immediately measured parallel to control cells in the following setting: basal respiration, respiration after addition of oligomycin (2 μg/ml final concentration), carbonyl cyanid p-(trifluoromethoxy)phenylhydrazone (1 μM), rotenone (2 μM), and finally KCN (2 mM). The quotient of basal respiration and respiration after oligomycin incubation was calculated and used as degree of the respiratory ratio.

Human Aβ 1–40 *ELISA and mouse* Aβ 1–40 *ELISA*

For the detection of secreted soluble mouse and human *Aβ 1–40 and Aβ 1–42*, a specific sandwich ELISA employing monoclonal antibodies was used. The ELISA was performed according to the instructions given in the Abeta-ELISA kit by Invitrogen. Briefly, to measure human basal soluble A$\beta_{1\text{-}40}$ and A$\beta_{1\text{-}42}$ levels, transfected HEK cells were allowed to grow until 80% confluence. Afterward, supernatants were collected and ELISA was conducted. Cell pellets were used for protein determination to normalize the samples. To detect A$\beta_{1\text{-}40}$ in HEKut cells, HEK cells were incubated with rotenone (25 μM) or antimycin (100 μM) for 2 or 24 h in the absence of presence of vitamin C (1000 μM). Afterward, supernatants were collected and after a centrifugation step (400 *g* for 5 min) and the ELISA was conducted. Cell pellets were used for protein determination to normalize the samples.

Ndufs4-null mice (KO) were generated as described elsewhere (21). All animal experiments were approved by the Animal Care and Use Committee at the University of Washington. Mice were maintained with rodent diet (5053; Picolab) and water available ad libitum with 12-h light–dark cycle at 22°C. At an age of 5 weeks, mice were anesthetized with an overdose of pentobarbital and whole brains were frozen in isopentane/dry ice, and stored at −80°C until use. The cerebellum was removed and the tissue was homogenized in eightfold-volume ice-cold buffer (phosphate-buffered saline [PBS]/protease inhibitor [PI]) of the brain weight and homogenized using a glass homogenizer (10–15 strokes, 400 rpm) The resulting homogenate was centrifuged at 15,000 *g* for 30 min at 4°C and directly transferred to the A$\beta_{1\text{-}40}$ mouse ELISA measurements using a Victor^2 multiplate reader (PerkinElmer Life Sciences). The protein content was determined according to the method of Lowry (29) using bovine serum albumin as the standard (BIO-RAD).

Heterozygous C57BL/6J mice (from Charles River) bearing the human Swedish mutation (KM670/671NL) and London mutation (V717I) in the 751 amino acid form of tgAPP under the control of a murine Thy1.2 promoter were bred in our animal facilities and were used in these experiments at an age of 13 months. All animal care and experimental procedures were in concordance with the German law on animal care and handling of transgenic animals. At weaning, the animals were genotyped from tail biopsies by means of an appropriate digest and polymerase chain reaction (data not shown).The mice were treated with rotenone 10 mg/kg/BW solubilized in

mygliol/dimethyl sulfoxide (2%) i.p. for 3 days. Afterward, animals were sacrificed by decaptation, and the brain hemispheres were rapidly dissected and washed in ice-cold buffer (PBS/PI). After removing the cerebellum, the tissue was homogenized in eightfold-volume ice-cold buffer (PBS/PI) of the brain weight homogenized using a glass homogenizer (10–15 strokes, 400 rpm), and the resulting homogenate was centrifuged at 15,000 *g* for 30 min at 4°C. The supernatant was diluted 1:50 in standard diluent buffer provided by Invitrogen, and $A\beta_{1\text{-}40}$ levels were determined using a specific human $A\beta_{1\text{-}40}$ ELISA (Invitrogen) using a Victor^2 multiplate reader (PerkinElmer Life Sciences). The protein content was determined according to the method of Lowry (29) using bovine serum albumin as the standard (BIO-RAD).

Confocal laser scanning microscopy

HEK cells were seeded 3 days before measurement on cover slips, which were coated with 0.01% gelatin. For live cell imaging experiments, cells were incubated overnight with 25 n*M* Mitotracker Deep Red. Micrographs were taken with a Leica SP 5 confocal laser scanning microscope (Leica) fitted with the appropriate filters and a plan-apochromate 63×, 1.4 NA. Live cell experiments were performed at 37°C and 5% CO_2 in a humidified chamber. For mitochondrial mobility studies, a picture was taken every 1.5 s over 2 min and the increase in gray scales was calculated compared to the first picture (23).

For morphological analyses, cells were incubated overnight with 25 n*M* Mitotracker CMXRos and fixed with 4% formalin in PBS (pH 7.4, 37°C) for 20 min at room temperature, washed three times with PBS, lysed for 30 min with 0.2% Triton ×100 solution, and washed three times with PBS. The samples were embedded in Mowiol and analyzed with the confocal laser scan microscope TCS SP5 (Leica). For analysis of mitochondrial dynamics, ImageJ 1.38× (National Institutes of Health) was used. For analyses of mitochondrial morphology, Imaris Version 6.2 (Bitplane) was used. AutoQuant X Version 2.1 from Media Cybernetics was used for deconvolution.

BACE1 activity

To determine basal BACE1 activity, HEK control, HEK APPwt, and APPsw cells were allowed to grow until 80% confluence. Cells were collected and resuspended in ice-cold extraction buffer. The resulting supernatant was used according to the instructions given in the β-Secretase Activity Assay Kit, Fluorogenic by Calbiochem. For normalization, protein levels of every probe were determined.

Statistical analysis

The data are given as the mean ± SEM. For statistical comparison, Student's *t*-test and one-way analysis of variance followed by Tukey's *post hoc* test for multiple comparisons were used. p-Values < 0.05 were considered statistically significant.

Acknowledgments

This work was supported by the HELMA (Helmholtz Alliance for Mental Health and Ageing) to M.W. and C.H., by the SFB 596 (M.W. and C.H.), by the DFG grant RE1575-1/1 (A.S.R. and A.O.), the Cluster of Excellence Frankfurt Macromolecular Complexes at the Goethe University Frankfurt DFG project EXC 115 (A.S.R. and U.B.), and the BMBF projects GerontoMitoSys 0315584A (A.S.R. and U.B.) and mitoNET 01GM0863 (I.W.).

Author Disclosure Statement

No competing interests exist.

References

1. Anandatheerthavarada HK and Devi L. Amyloid precursor protein and mitochondrial dysfunction in Alzheimer's disease. *Neuroscientist* 13: 626–638, 2007.
2. Andreyev AI, Kushnareva YE, and Starkov AA. Mitochondrial metabolism of reactive oxygen species. *Biochem Mosc* 70: 200–214, 2005.
3. Behl C. Apoptosis and Alzheimer's disease. *J Neural Transm* 107: 1325–1344, 2000.
4. Benard G, Bellance N, James D, Parrone P, Fernandez H, Letellier T, and Rossignol R. Mitochondrial bioenergetics and structural network organization. *J Cell Sci* 120: 838–848, 2007.
5. Bishop NA, Lu T, and Yankner BA. Neural mechanisms of ageing and cognitive decline. *Nature* 464: 529–535, 2010.
6. Blalock EM, Chen KC, Sharrow K, Herman JP, Porter NM, Foster TC, and Landfield PW. Gene Microarrays in hippocampal aging: statistical profiling identifies novel processes correlated with cognitive impairment. *J Neurosci* 23: 3807–3819, 2003.
7. Cai H, Wang Y, McCarthy D, Wen H, Borchelt DR, Price DL, and Wong PC. BACE1 is the major beta-secretase for generation of Abeta peptides by neurons. *Nat Neurosci* 4: 233–234, 2001.
8. Choi WS, Kruse SE, Palmiter RD, and Xia ZG. Mitochondrial complex I inhibition is not required for dopaminergic neuron death induced by rotenone, MPP+, or paraquat. *Proc Natl Acad Sci U S A* 105: 15136–15141, 2008.
9. David DC, Hauptmann S, Scherping I, Schuessel K, Keil U, Rizzu P, Ravid R, Drose S, Brandt U, Muller WE, Eckert A, and Gotz J. Proteomic and functional analyses reveal a mitochondrial dysfunction in P301L Tau transgenic mice. *J Biol Chem* 280: 23802–23814, 2005.
10. Devi L, Prabhu BM, Galati DF, Avadhani NG, and Anandatheerthavarada HK. Accumulation of amyloid precursor protein in the mitochondrial import channels of human Alzheimer's disease brain is associated with mitochondrial dysfunction. *J Neurosci* 26: 9057–9068, 2006.
11. Du H, Guo L, Yan SQ, Sosunov AA, McKhann GM, and Yan SS. Early deficits in synaptic mitochondria in an Alzheimer's disease mouse model. *Proc Natl Acad Sci U S A* 107: 18670–18675, 2010.
12. Eckert A, Steiner B, Marques C, Leutz S, Romig H, Haass C, and Muller WE. Elevated vulnerability to oxidative stress-induced cell death and activation of caspase-3 by the Swedish amyloid precursor protein mutation. *J Neurosci Res* 64: 183–192, 2001.
13. Finsterer J. Mitochondrial disorders, cognitive impairment and dementia. *J Neurol Sci* 283: 143–148, 2009.
14. Fukui H, Diaz F, Garcia S, and Moraes CT. Cytochrome c oxidase deficiency in neurons decreases both oxidative stress and amyloid formation in a mouse model of Alzheimer's disease. *Proc Natl Acad Sci U S A* 104: 14163–14168, 2007.
15. Fukumoto H, Cheung BS, Hyman BT, and Irizarry MC. Beta-secretase protein and activity are increased in the

neocortex in Alzheimer disease. *Arch Neurol* 59: 1381–1389, 2002.
16. Guglielmotto M, Aragno M, Autelli R, Giliberto L, Novo E, Colombatto S, Danni O, Parola M, Smith MA, Perry G, Tamagno E, and Tabaton M. The up-regulation of BACE1 mediated by hypoxia and ischemic injury: role of oxidative stress and HIF1 alpha. *J Neurochem* 108: 1045–1056, 2009.
17. Haass C and Selkoe DJ. Soluble protein oligomers in neurodegeneration: lessons from the Alzheimer's amyloid beta-peptide. *Nat Rev Mol Cell Biol* 8: 101–112, 2007.
18. Hauptmann S, Scherping I, Drose S, Brandt U, Schulz KL, Jendrach M, Leuner K, Eckert A, and Muller WE. Mitochondrial dysfunction: an early event in Alzheimer pathology accumulates with age in AD transgenic mice. *Neurobiol Aging* 30: 1574–1586, 2009.
19. Holsinger RM, McLean CA, Beyreuther K, Masters CL, and Evin G. Increased expression of the amyloid precursor beta-secretase in Alzheimer's disease. *Ann Neurol* 51: 783–786, 2002.
20. Holsinger RM, McLean CA, Collins SJ, Masters CL, and Evin G. Increased beta-Secretase activity in cerebrospinal fluid of Alzheimer's disease subjects. *Ann Neurol* 55: 898–899, 2004.
21. Hutter E, Unterluggauer H, Garedew A, Jansen-Durr P, and Gnaiger E. High-resolution respirometry—a modern tool in aging research. *Exp Gerontol* 41: 103–109, 2006.
22. Jendrach M, Mai S, Pohl S, Voth M, and Bereiter-Hahn J. Short- and long-term alterations of mitochondrial morphology, dynamics and mtDNA after transient oxidative stress. *Mitochondrion* 8: 293–304, 2008.
23. Jendrach M, Pohl S, Voth M, Kowald A, Hammerstein P, and Bereiter-Hahn J. Morpho-dynamic changes of mitochondria during ageing of human endothelial cells. *Mech Ageing Dev* 126: 813–821, 2005.
24. Kaido M, Fujimura H, Soga F, Toyooka K, Yoshikawa H, Nishimura T, Higashi T, Inui K, Imanishi H, Yorifuji S, and Yanagihara T. Alzheimer-type pathology in a patient with mitochondrial myopathy, encephalopathy, lactic acidosis and stroke-like episodes (MELAS). *Acta Neuropathol* 92: 312–318, 1996.
25. Keil U, Bonert A, Marques CA, Scherping I, Weyermann J, Strosznajder JB, Muller-Spahn F, Haass C, Czech C, Pradier L, Muller WE, and Eckert A. Amyloid beta-induced changes in nitric oxide production and mitochondrial activity lead to apoptosis. *J Biol Chem* 279: 50310–50320, 2004.
26. Kruse SE, Watt WC, Marcinek DJ, Kapur RP, Schenkman KA, and Palmiter RD. Mice with mitochondrial complex I deficiency develop a fatal encephalomyopathy. *Cell Metabol* 7: 312–320, 2008.
27. Kushnareva Y, Murphy AN, and Andreyev A. Complex I-mediated reactive oxygen species generation: modulation by cytochrome c and NAD(P)+ oxidation-reduction state. *Biochem J* 368: 545–553, 2002.
28. Li Q and Sudhof TC. Cleavage of amyloid-beta precursor protein and amyloid-beta precursor-like protein by BACE 1. *J Biol Chem* 279: 10542–10550, 2004.
29. Lowry OH, Rosebrough NJ, Farr AL, and Randall RJ. Protein Measurement with the Folin Phenol Reagent. *J Biol Chem* 193: 265–275, 1951.
30. Lu T, Pan Y, Kao SY, Li C, Kohane I, Chan J, and Yankner BA. Gene regulation and DNA damage in the ageing human brain. *Nature* 429: 883–891, 2004.
31. Luo Y, Bolon B, Kahn S, Bennett BD, Babu-Khan S, Denis P, Fan W, Kha H, Zhang J, Gong Y, Martin L, Louis JC, Yan Q, Richards WG, Citron M, and Vassar R. Mice deficient in BACE1, the Alzheimer's beta-secretase, have normal phenotype and abolished beta-amyloid generation. *Nat Neurosci* 4: 231–232, 2001.
32. Manczak M, Jung Y, Park BS, Partovi D, and Reddy PH. Time-course of mitochondrial gene expressions in mice brains: implications for mitochondrial dysfunction, oxidative damage, and cytochrome c in aging. *J Neurochem* 92: 494–504, 2005.
33. Mattson MP. Pathways towards and away from Alzheimer's disease. *Nature* 430: 631–639, 2004.
34. Mattson MP. Neuronal life-and-death signaling, apoptosis, and neurodegenerative disorders. *Antioxid Redox Signal* 8: 1997–2006, 2006.
35. Mattson MP. Mitochondrial regulation of neuronal plasticity. *Neurochem Res* 32: 707–715, 2007.
36. Mattson MP, Barger SW, Begley JG, and Mark RJ. Calcium, free radicals, and excitotoxic neuronal death in primary cell culture. *Methods Cell Biol* 46: 187–216, 1995.
37. Mattson MP, Gleichmann M, and Cheng A. Mitochondria in neuroplasticity and neurological disorders. *Neuron* 60: 748–766, 2008.
38. Mattson MP and Magnus T. Ageing and neuronal vulnerability. *Nat Rev Neurosci* 7: 278–294, 2006.
39. Müller WE, Eckert A, Kurz C, Eckert GP, and Leuner K. Mitochondrial dysfunction: common final pathway in brain aging and Alzheimer's disease—therapeutic aspects. *Mol Neurobiol* 41: 159–171, 2010.
40. Nakahara H, Kanno T, Inai Y, Utsumi K, Hiramatsu M, Mori A, and Packer L. Mitochondrial dysfunction in the senescence accelerated mouse (SAM). *Free Radic Biol Med* 24: 85–92, 1998.
41. Navarro A and Boveris A. Brain mitochondrial dysfunction in aging: conditions that improve survival, neurological performance and mitochondrial function. *Front Biosci* 12: 1154–1163, 2007.
42. O'Connor T, Sadleir KR, Maus E, Velliquette RA, Zhao J, Cole SL, Eimer WA, Hitt B, Bembinster LA, Lammich S, Lichtenthaler SF, Hebert SS, De Strooper B, Haass C, Bennett DA, and Vassar R. Phosphorylation of the translation initiation factor eIF2alpha increases BACE1 levels and promotes amyloidogenesis. *Neuron* 60: 988–1009, 2008.
43. Paradies G, Petrosillo G, Paradies V, and Ruggiero FM. Oxidative stress, mitochondrial bioenergetics, and cardiolipin in aging. *Free Radic Biol Med* 48: 1286–1295, 2010.
44. Pavlov PF, Petersen CH, Glaser E, and Ankarcrona M. Mitochondrial accumulation of APP and Abeta: significance for Alzheimer disease pathogenesis. *J Cell Mol Med* 3: 4137–4145, 2009.
45. Petrosillo G, Matera M, Casanova G, Ruggiero FM, and Paradies G. Mitochondrial dysfunction in rat brain with aging Involvement of complex I, reactive oxygen species and cardiolipin. *Neurochem Int* 53: 126–131, 2008.
46. Querfurth HW and LaFerla FM. Alzheimer's disease. *N Engl J Med* 362: 329–344, 2010.
47. Reddy PH. Amyloid beta, mitochondrial structural and functional dynamics in Alzheimer's disease. *Exp Neurol* 218: 286–292, 2009.
48. Reddy PH, Manczak M, Mao P, Calkins MJ, Reddy AP, and Shirendeb U. Amyloid-beta and mitochondria in aging and Alzheimer's disease: implications for synaptic damage and cognitive decline. *J Alzheimers Dis* 20 Suppl 2: S499–S512, 2010.
49. Rhein V, Song XM, Wiesner A, Ittner LM, Baysang G, Meier F, Ozmen L, Bluethmann H, Drose S, Brandt U, Savaskan E,

Czech C, Gotz J, and Eckert A. Amyloid-beta and tau synergistically impair the oxidative phosphorylation system in triple transgenic Alzheimer's disease mice. *Proc Natl Acad Sci U S A* 106: 20057–20062, 2009.
50. Salsano E, Giovagnoli AR, Morandi L, Maccagnano C, Lamantea E, Marchesi C, Zeviani M, and Pareyson D. Mitochondrial dementia: a sporadic case of progressive cognitive and behavioral decline with hearing loss due to the rare m.3291T>C MELAS mutation. *J Neurol Sci* 300: 165–168, 2011.
51. Su B, Wang XL, Bonda D, Perry G, Smith M, and Zhu XW. Abnormal Mitochondrial Dynamics-A Novel Therapeutic Target for Alzheimer's Disease? *Mol Neurobiol* 41: 87–96, 2010.
52. Su B, Wang XL, Zheng L, Perry G, Smith MA, and Zhu XW. Abnormal mitochondrial dynamics and neurodegenerative diseases. *Biochim Biophys Acta* 1802: 135–142, 2010.
53. Sun X, He G, Qing H, Zhou W, Dobie F, Cai F, Staufenbiel M, Huang LE, and Song W. Hypoxia facilitates Alzheimer's disease pathogenesis by up-regulating BACE1 gene expression. *Proc Natl Acad Sci U S A* 103: 18727–18732, 2006.
54. Swerdlow RH and Kish SJ. Mitochondria in Alzheimer's disease. *Int Rev Neurobiol* 53: 341–385, 2002.
55. Tamagno E, Guglielmotto M, Aragno M, Borghi R, Autelli R, Giliberto L, Muraca G, Danni O, Zhu XW, Smith MA, Perry G, Jo DG, Mattson MP, and Tabaton M. Oxidative stress activates a positive feedback between the gamma- and beta-secretase cleavages of the beta-amyloid precursor protein. *J Neurochem* 104: 683–695, 2008.
56. Tamagno E, Parola M, Bardini P, Piccini A, Borghi R, Guglielmotto M, Santoro G, Davit A, Danni O, Smith MA, Perry G, and Tabaton M. Beta-site APP cleaving enzyme up-regulation induced by 4-hydroxynonenal is mediated by stress-activated protein kinases pathways. *J Neurochem* 92: 628–636, 2005.
57. Verkaart S, Koopman WJH, Cheek J, Emst-de Vries SE, van den Heuvel LWPJ, Smeitink JAM, and Willems PHGM. Mitochondrial and cytosolic thiol redox state are not detectably altered in isolated human NADH: ubiquinone oxidoreductase deficiency. *Biochim Biophys Acta* 1772: 1041–1051, 2007.
58. Wang X, Su B, Lee HG, Li X, Perry G, Smith MA, and Zhu X. Impaired balance of mitochondrial fission and fusion in Alzheimer's disease. *J Neurosci* 29: 9090–9103, 2009.
59. Wang X, Su B, Siedlak SL, Moreira PI, Fujioka H, Wang Y, Casadesus G, and Zhu X. Amyloid-beta overproduction causes abnormal mitochondrial dynamics via differential modulation of mitochondrial fission/fusion proteins. *Proc Natl Acad Sci U S A* 105: 19318–19323, 2008.
60. Yang LB, Lindholm K, Yan R, Citron M, Xia W, Yang XL, Beach T, Sue L, Wong P, Price D, Li R, and Shen Y. Elevated beta-secretase expression and enzymatic activity detected in sporadic Alzheimer disease. *Nat Med* 9: 3–4, 2003.
61. Yao J, Irwin RW, Zhao L, Nilsen J, Hamilton RT, and Brinton RD. Mitochondrial bioenergetic deficit precedes Alzheimer's pathology in female mouse model of Alzheimer's disease. *Proc Natl Acad Sci U S A* 106: 14670–14675, 2009.

Address correspondence to:
Prof. Kristina Leuner
Department of Pharmacology
ZAFES, Biocenter
University of Frankfurt, Frankfurt/Main
Max-von-Laue-Str.9
60438 Frankfurt
Germany

E-mail: leuner@em.uni-frankfurt.de

Date of first submission to ARS Central, July 27, 2011; date of final revised submission, December 23, 2011; date of acceptance, January 02, 2012.

Abbreviations Used

Aβ = amyloid beta
AD = Alzheimer's disease
ADAM = a disintegrin and metalloprotease domain
APP = amyloid precursor protein
APPsw = APP containing the Swedish mutation
APPwt = wild-type APP
BACE1 = β-site APP cleaving enzyme
BW = body weight
complex IV = cytochrome c oxidase
DHE = dihydroethidium
DHR = dihydrorhodamin
ELISA = enzyme-linked immunosorbent assay
HBSS = Hanks' balanced salt solution
HEKut = untransfected human embryonic kidney cells
MELAS = mitochondrial encephalopathy, lactatacidosis, stroke-like episodes
MFI = mean fluorescence intensity
MMP = mitochondrial membrane potential
KO = knockout
PBS = phosphate-buffered saline
PD = Parkinson disease
PI = protease inhibitor
R123 = Rhodamine 123
RCR = respiratory control ratio
ROS = reactive oxygen species
rot = rotenone
SEM = standard error of the mean
tgAPP = human APP
TOM = translocase of the outer mitochondrial membrane